# Electrospun scaffolds from silk fibroin and their cellular compatibility

**Kuihua Zhang,[1,2,3,4] Xiumei Mo,[1,2,3] Chen Huang,[1,2] Chuanglong He,[1,2] Hongsheng Wang[1,2]**

[1]*Key Laboratory of Textile Science and Technology, Ministry of Education, DongHua University, Shanghai 201620, China*

[2]*Biomaterials and Tissue Engineering Laboratory, College of Chemistry and Chemical Engineering and Biological Engineering, DongHua University, 2999 Renmin Rd. North, Songjiang District, Shanghai 201620, China*

[3]*State Key Laboratory for Modification of Chemical Fibers and Polymer Materials, College of Materials Science and Engineering, DongHua University, Shanghai 201620, China*

[4]*College of Biological Engineering and Chemical Engineering, Jiaxing College, Zhejiang 314001, China*

Received 3 February 2009; accepted 4 February 2009
Published online 31 August 2009 in Wiley InterScience (www.interscience.wiley.com). DOI: 10.1002/jbm.a.32497

**Abstract:** Electrospinning offers an attractive opportunity for producing silk fibroin (SF) nano/micro fibrous scaffolds with potential for tissue regeneration and repair. Electrospun scaffolds of silk fibroin were fabricated as a biomimetic scaffold for tissue engineering. The morphology of the electrospun scaffolds was investigated with SEM and AFM. The SEM images indicated that electrospun SF fibers were ribbon-shaped and the average width increased with increasing SF concentrations. The AFM images revealed that, after treated with methanol, there was a groove on the surface of fiber, which is conducive to cell attachment. The structure of electrospun SF fibers was characterized by NMR, WAXD, and DSC. The results displayed that SF in electrospun fibers was present in a random coil conformation, SF conformation transformed from random coil to β-sheet when treated with methanol. Cell attachment and proliferation studies with pig iliac endothelial cells (PIECs) demonstrated that electrospun SF scaffolds significantly promoted cell attachment and proliferation in comparison with cast SF films. These results suggest electrospun SF scaffolds may be potential candidates for cardiovascular tissue engineering. © 2009 Wiley Periodicals, Inc. J Biomed Mater Res 93A: 976–983, 2010

**Key words:** silk fibroin; electrospinning; aqueous solution; tissue engineering

## INTRODUCTION

Silk fibroin (SF) is a main component of silkworm silk as well as an attractive natural fibrous protein for biomedical applications due to several unique properties, including good biocompatibility, good oxygen and water vapor permeability, and biodegradability, low inflammatory response, and good mechanical properties.[1,2] Recently, electrospinning silk fibroin to mimic the natural ECM has gained interest from researchers. SF has been electrospun with the spinning solvents such as hexafluoro-2-propanol (HFIP),[3,4] hexafluoroacetone (HFA),[5] and formic acid.[6,7] These organic solvents are toxic and unfriendly to humans and the environment. A trace of toxic organic solvents or acids could exist in electrospun scaffolds for tissue engineering, which will affect cytocompatibility. To enhance the electrospinnability of aqueous SF solutions, Electrospinning from aqueous SF solutions mixed with poly (ethylene oxide) (PEO) was established and fiber morphology showed uniform fibers less than 800 nm in diameter.[8] The human aortic endothelial cell (HAEC) and human coronary artery smooth muscle cell (HCASMC) cultured on these scaffolds showed good attachment and proliferation.[9] However, adding a large quantity of the water-soluble PEO will eventually affect the structural integrity and stability. Hence, researchers have made efforts to electrospin

*Correspondence to:* X. Mo; e-mail: xmm@dhu.edu.cn

Contract grant sponsor: National Science Foundation; contract grant number: 30570503

Contract grant sponsor: National High Technology Research and Developed Program (863 Program); contract grant number: 2008AA03Z305

Contract grant sponsor: Science and Technology Commission of Shanghai Municipality Program; contract grant numbers: 08520704600, 0852nm03400

Contract grant sponsor: "111 Project" Biomedical Textile Materials Science and Technology; contract grant number: B07024

all-aqueous SF solutions.[10,11] However, from the dialyzed SF aqueous solutions (ca. 2 wt %) to an electrospinnable concentration, the process needs longer time and lower temperature, otherwise, SF aqueous solutions would easily generate gels.[12] Furthermore, the processing details and the potential applications of those fibers for tissue engineering have not been fully explored.

In this study, the regenerated SF aqueous solutions of different concentration generated through the lyophilized regenerated SF sponges were electrospun. The morphology and structure were also investigated. To assess the cytocompatibility and cells behavior on electrospun scaffolds, interaction between electrospun silk fibroin scaffolds with living cells was studied and compared with cast films.

## MATERIALS AND METHODS

### Materials

Cocoons of *Bombyx mori* silkworm were kindly supplied by Jiaxing Silk Co. (China). Pig iliac endothelial cells (PIECs) were obtained from institute of biochemistry and cell biology (Chinese Academy of Sciences, China). Culture media and reagents were purchased from Gibco Life Technologies CO.

### Preparation of regenerated SF

Cocoons were degummed three times in 0.5% (w/w) $Na_2CO_3$ solution at 100°C for 30 min each and then rinsed thoroughly with distilled water to extract the glue-like sericin proteins. Degummed silk was dissolved in a ternary-solvent system of $CaCl_2/H_2O/C_2H_5OH$ solution (1:8:2 in molar ratio) at 70°C for 1 h. The silk solution was dialyzed against distilled water using cellulose tube (250-7u, Sigma) at room temperature for 3 days. Then, the SF solution was filtered and lyophilized to obtain the regenerated SF sponges.

### Electrospinning of SF ultrafine fibrous scaffolds

SF solutions were prepared by dissolving the regenerated SF sponges in distilled water for 6 h. Concentrations of SF solutions ranged from 15 to 40 wt %. The SF aqueous solutions were filled into a 2.5 mL plastic syringe with a blunt-ended needle. The syringe was located in a syringe pump (789100C, Cole-Pamer, America) and dispensed at a rate of 0.5 mL/h. A voltage of 20 kV using a high voltage power supply (BGG6-358, BMEICO.LTD. China) was applied across the needle and ground collector, which was placed at a distance of 20 cm. Electrospun SF scaffolds were immersed into pure methanol solution for 10 min to induce β-sheet conformational transition and then dried under vacuum at room temperature for 24 h.

### Characterization

The morphology was observed with a scanning electronic microscope (SEM) (JSM-5600, Japan) at an accelerated voltage of 10 kV. The mean fiber widths were estimated using an image analysis software (Image-J, National Institutes of Health) and calculated by selecting 100 fibers randomly observed on the SEM images. Fiber surface topography was inspected with an atomic force microscope (AFM) (Nanoscope IV, America).

The $^{13}C$ CP-MAS NMR spectra of SF scaffolds were obtained on NMR spectrometer (Bruker AV400, Switzerland) with a $^{13}C$ resonance frequency of 100 MHz, contact time of 1.0 ms, and pulse delay time of 4.0 s.

Wide-angle X-ray diffraction (WAXD) curves were obtained on an X-ray diffractometer (Riga Ku, Japan) within the scanning region of 2θ (5°–50°), with Cu $K_\alpha$ radiation ($\lambda = 1.5418$ Å) at 40 kV and 40 mA.

The thermographs were acquired using a differential scanning calorimeter (TA Instruments Co.) from room temperature to 330°C at a rate of 10°C/min under a nitrogen atmosphere. The nitrogen gas flow rate was 40 mL/min.

### Viability study of PIECs on SF scaffolds

Pig iliac endothelial cells (PIECs) were cultured in DMEM medium with 10% fetal bovine serum and 1% antibiotic-antimycotic solution. The medium was replaced every 2 days and the cultures were maintained in a humidified incubator at 37°C and 5% $CO_2$. Electrospun SF scaffolds and solvent-cast films were prepared on circular glass coverslips with a diameter of 14 mm and fixed in 24-well cell culture plates with stainless rings. Before seeding cells, scaffolds were sterilized by 75% ethanol for 2 h and washed three times with phosphate-buffered saline solution (PBS), and then washed once with the culture medium.

Cell viability on the electrospun SF fibrous scaffolds, cast films, and coverslips (control) was determined by MTT method. Briefly, the cells and SF scaffolds were incubated with 5 mg/mL 3-[4, 5-dimehyl-2-thiazolyl]-2, 5-diphenyl-2H-tetrazolium bromide (MTT) containing serum free medium at 37°C and 5% $CO_2$ for 4 h. Thereafter, the culture media were extracted and 400 μL dimethylsulfoxide (DMSO) added for about 20 min. When the crystals were sufficiently resolved, aliquots were pipetted into the wells of a 96-well plate and tested by an Enzyme-labeled Instrument (MK3, Thermo), and the absorbance at 490 nm for each well was measured.

For the attachment study, endothelial cells were seeded onto fibrous scaffolds, cast films and control glass coverslips ($n = 3$) at a density of $1.5 \times 10^4$ cells/well for 1, 2, 4, and 6 h. For the proliferation study, endothelial cells were seeded onto fibrous scaffolds, cast films, and control glass coverslips ($n = 3$) at a density of 8000 cells/well for 1, 3, 5, and 7 days. After cell seeding, unattached cells were washed out with PBS solution and attached cells were quantified by MTT method.

After 1 and 7 days of culturing, the electrospun fibrous scaffolds with cells (density is $1.5 \times 10^4$ cells/well) were

examined by SEM. The scaffolds were rinsed twice with PBS and fixed in 4% glutaraldehyde water solution at 4°C for 2 h. Fixed samples were rinsed twice with PBS dehydrated in graded concentrations of ethanol (30, 50, 70, 80, 90, 95, and 100%), and dried in vacuum overnight. The dry cellular constructs were coated with gold sputter and observed under the SEM.

### Statistical analysis

Statistical analysis was performed using Origin 7.5 (Origin Lab). Statistical comparisons were determined by the analysis of One-Way ANOVA. In all evaluations, $p < 0.05$ was considered as statistically significant.

## RESULTS AND DISCUSSION

### Morphology of SF ultrafine fibers

The morphology of fibers varied with concentrations of the SF aqueous solutions. Fibers were not obtained at concentrations of 15 wt % or below because a stable cone at the end of spinneret was not maintained. The SEM micrographs and average widths of ultrafine fibers from the SF aqueous solutions with different concentrations ranging from 20 to 35 wt % are shown in Figures 1 and 2. The morphology of electrospun fibers from all concentrations was ribbon-shaped. According to Koombhongse et al.,[13] ribbon-shaped fibers are obtained due to the formation of a thin polymer shell on the surface of the cylindrical fluid jet between the electrodes. The solvent evaporates after shell formation, atmospheric pressure causes a collapse of the cylindrical jet, and the fibers change first into an elliptic and then into a flat shape. Incomplete fiber drying also leads to the formation of ribbon-like (or flattened) fibers when compared with fibers with a circular cross section. At the 20 wt % concentration, beaded fibers are generated by electrospinning due to the lower polymer concentration, which is not sufficient to produce an adequate viscosity for chain entanglements. Dietzel et al.[14] demonstrated that solution surface tension and viscosity play important roles in determining the range of concentrations from which continuous fibers can be obtained in electrospinning. With an increase in SF concentration, morphology appears to change gradually from fibers with spindle-like beads to uniform fibers, and the average widths of fibers increased gradually. Their average widths were 234, 343, 890, and 1016 nm, respectively. At 40 wt % concentration, the electrospinning process was not possible due to the viscosity of the SF solution.

The SEM micrographs of the electrospun SF fibers (untreated) and the electrospun SF fibers (treated with methanol) are shown in Figure 3. After methanol treatment, the surface of electrospun SF fibers became rougher. To further demonstrate the surface

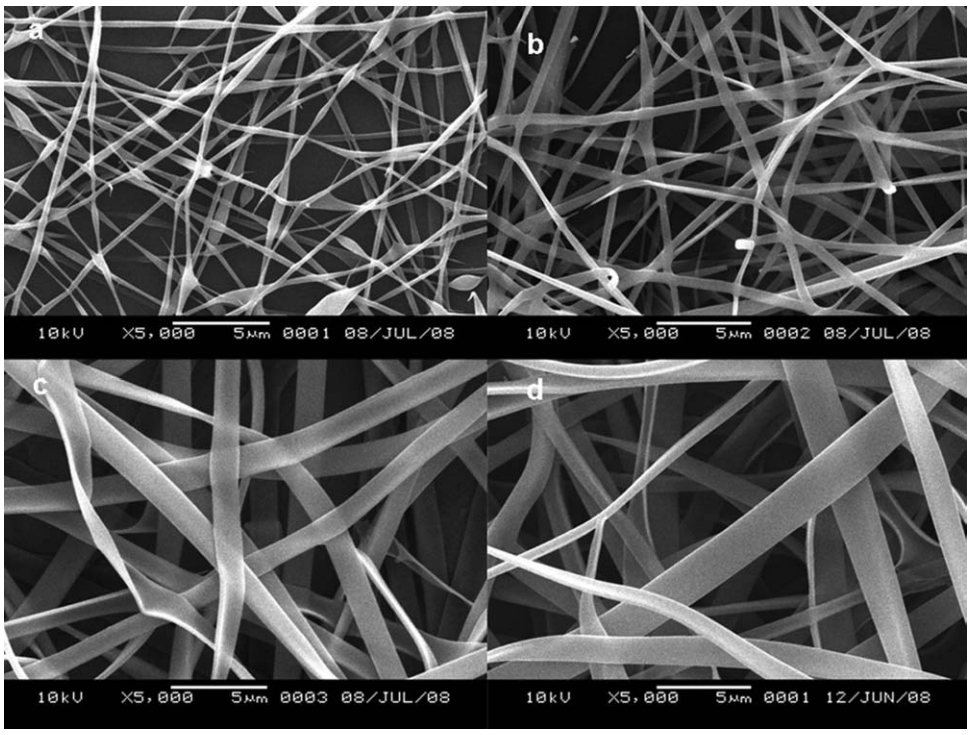


**Figure 1.** SEM micrographs of electrospun SF fibers with concentrations of (a) 20 wt %, (b) 25 wt %, (c) 30 wt %, and (d) 35 wt %.

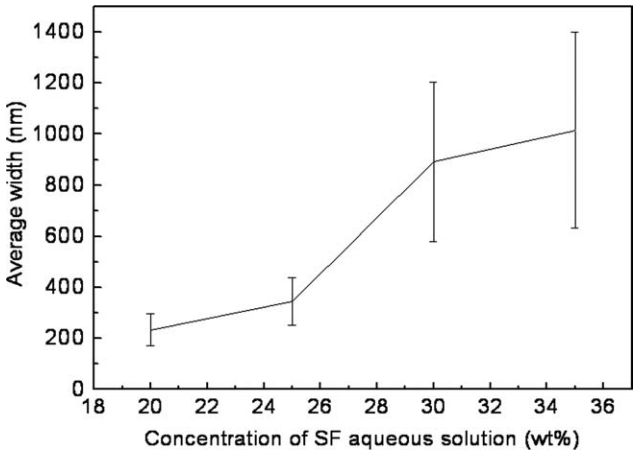


**Figure 2.** Dependence of the widths of electrospun SF fibers on the concentrations of SF aqueous solutions. The error bar representing standard deviation.

topographies of the electrospun SF fibers (untreated) and the electrospun SF fibers (methanol treated), AFM images were examined Figure 4. From the analysis of AFM, we also found that the surface of the electrospun SF fibers (untreated) is smooth but the surface of the electrospun SF fiber treated with methanol has a groove, which was possibly due to the change of SF conformation from random coil to β-sheet structure in the methanol treatment process. Furthermore, this groove is conducive to cell adhesion.[15]

### The secondary structure of SF ultrafine fibers

Recently, solid-state $^{13}C$ NMR has been shown to be an effective analytical tool for demonstrating the formation of β-sheets in polypeptides and proteins due to the sensitivity of isotropic $^{13}C$ NMR chemical shifts of carbon atoms to the secondary structure. The secondary structure of *Bombyx mori* silk fibroin consists of the major conformations including random coils or helix (silk I) and β-sheet (silk II).[16] The β-sheet form can be identified by the $^{13}C$ chemical shifts of Gly (glycine), Ser (serine), and Ala (alanine) that are indicative of β-sheet conformations. Particularly, the chemical shift of alanyl $C^{\beta}$ is an excellent indicator of the silk fibroin conformation. Zhou et al.[17] illustrated that the chemical shifts in Ala residues of $C^{\beta}$ within 18.5–20.5 ppm were assigned β-sheet conformation (silk II), the chemical shifts in Ala residues of $C^{\beta}$ within 14.5–17.5 ppm were assigned random coils or helix (silk I). The higher chemical shifts in Ala residues of $C^{\beta}$ indicated more content of β-sheet conformation.[18] The $^{13}C$ NMR spectra of degummed SF, lyophilized SF sponge, electrospun SF scaffolds, and electrospun SF scaffolds treated with methanol are shown in Figure 5. The chemical shifts of Ala $C^{\beta}$ were 20.70, 16.75, 16.26, and 19.97 ppm, respectively. These results indicate that the degummed SF and electrospun SF scaffolds treated with methanol are mainly in a β-sheet conformation. However, the lyophilized SF sponge and electrospun SF scaffolds can be assigned a random coil conformation. The structure of electrospun fibrous scaffolds from all aqueous solutions was predominantly random coil. With methanol treatment, the random coil conformation converted to β-sheet conformation.

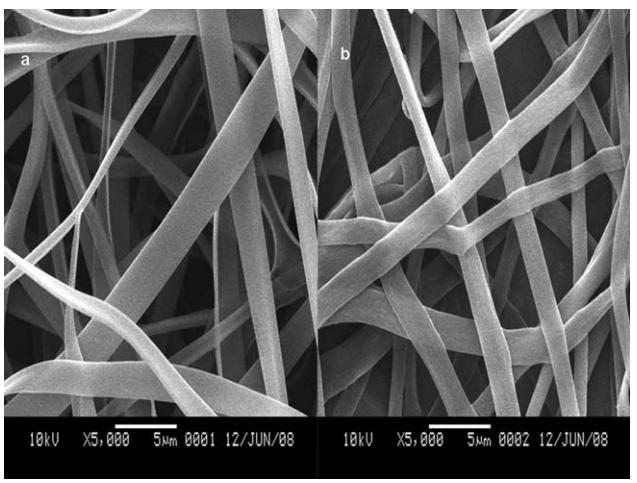


**Figure 3.** SEM micrographs of electrospun SF fibers (a) and electrospun SF fibers treated with methanol (b).

The WAXD spectra and crystallinities of degummed SF, lyophilized SF sponge, electrospun SF scaffolds without/with methanol treatment are shown in Figure 6 and Table I. X-ray diffraction analysis of degummed SF showed peaks at 9.0°, 20.6°, 24.7°, 29.0°, respectively. These peaks are similar to those of the β-sheet crystalline structure (silk II) of native silk fibroin.[19] The WAXD patterns of lyophilized SF sponge, electrospun SF scaffolds exhibited only a broad of peak centered at 22.8°, which is the characteristic peak of silk I. X-ray diffraction analysis of electrospun SF scaffolds treated with methanol showed peaks at 20.9°, 23.6°, respectively. These peaks are similar to the peaks of degummed SF. The results clarified that electrospun SF scaffolds from aqueous solutions are mainly in a random coil conformation (silk I), and only after methanol treatment do they convert to a β-sheet crystalline structure (silk II).

The thermographs of the SF matrices are shown in Figure 7. The samples exhibited two endothermic peaks around 75 and 290°C. The former peak is attributed to the evaporation of water and the latter peak is attributed to the destruction of SF. For the lyophilized SF sponge and electrospun SF scaffolds, the appearance of endothermic peaks at 178.5°C and 174.5°C are due to the glass transition of amorphous

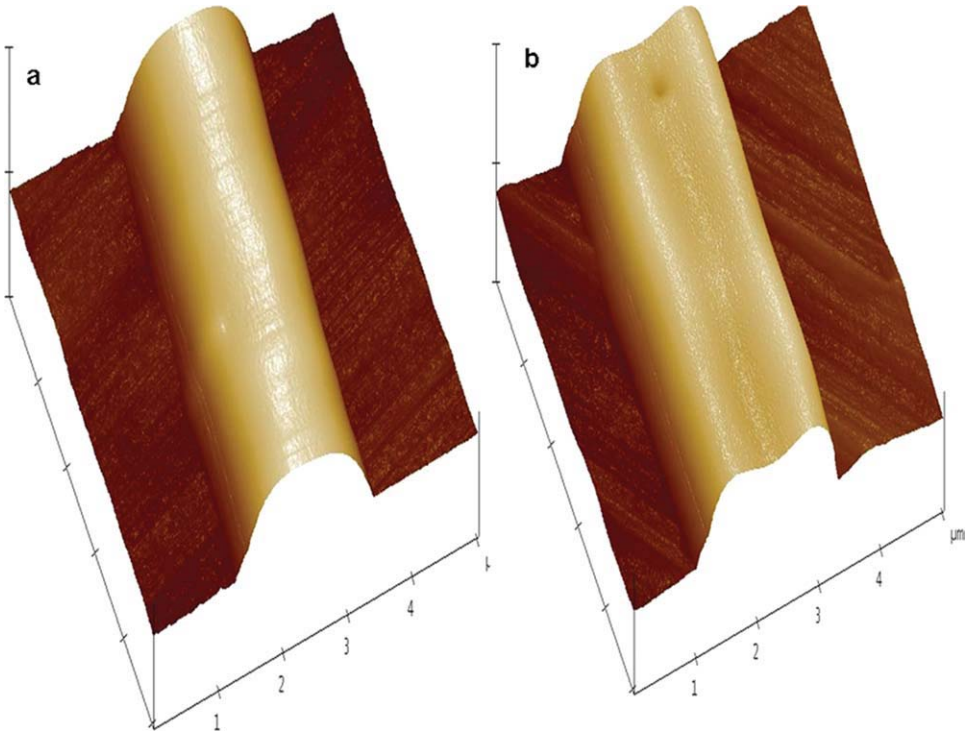


**Figure 4.** AFM images represented by height mode. (a) Electrospun SF fiber and (b) electrospun SF fiber treated with methanol. [Color figure can be viewed in the online issue, which is available at www.interscience.wiley.com.]

SF, respectively. The small exothermic peaks at 232.2 and 325.9°C are due to crystallization of amorphous SF with the accompanying conformation transition from random coil to β-sheet.[20] However, for the degummed SF and the electrospun SF scaffolds treated with methanol, no exothermic peak was observed until the decomposition temperature. This is because their initial structures are β-sheet. The thermo analytical results are consistent with the

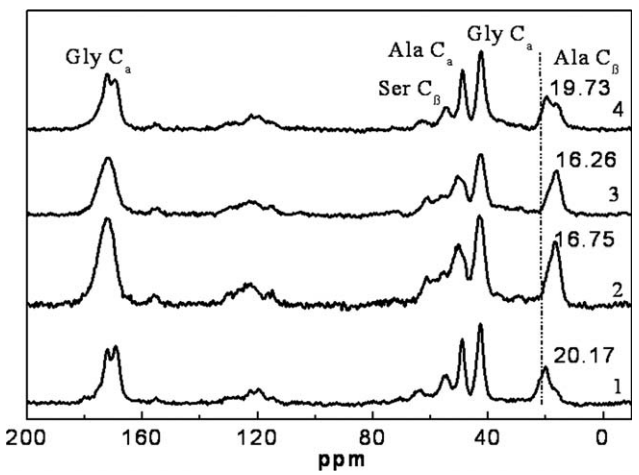


**Figure 5.** $^{13}C$ CP/MAS NMR spectra of SF matrices. 1-degummed silk, 2-lyophilized sponge, 3-electrospun scaffolds, and 4-electrospun scaffolds treated with methanol.

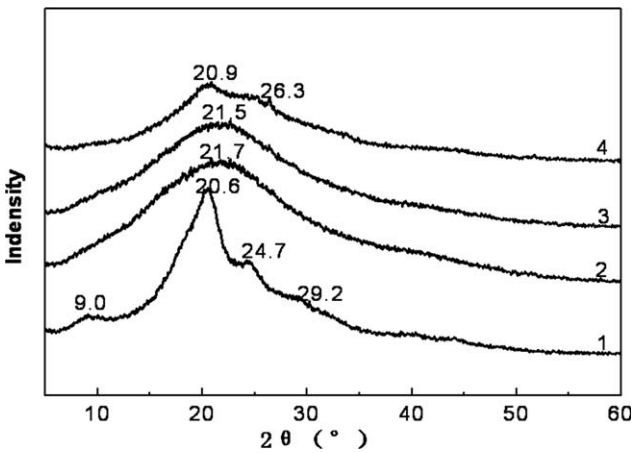


**Figure 6.** WAXD curves of SF matrices. 1-degummed silk, 2-lyophilized sponge, 3-electrospun scaffolds, and 4-electrospun scaffolds treated with methanol.

**TABLE I**
**Crystallinity of Silk Fibroin Acquired from Different Process**

| Type of SF | Crystallinity (%) |
|---|---|
| Degumed silk | 34.4 |
| Lyophilized sponge | 19.8 |
| Electrospun scaffolds | 16.9 |
| Electrospun scaffolds treated with methanol | 25.0 |

results from the NMR and WAXD characterization studies.

### Viability of cells on electrospun SF scaffolds

Scaffolding materials for tissue engineering approaches are typically designed to promote cell growth, physiological function, and the maintenance of the normal states of cell differentiation.[21] Electrospun SF scaffolds from aqueous solutions without the use of toxic organic solvents are beneficial to the cytocompatibility of SF scaffolds. Since both the topography and the porosity of scaffolds play significant roles in the attachment and proliferation of mammalian cells, the biocompatibility of the electrospun SF scaffolds was compared with the solvent-cast films and coverslips (control). Both attachment and proliferation of PIECs seeded on electrospun scaffolds, cast films, and coverslips (control) are graphically shown in Figures 8 and 9. Cell attachment on electrospun SF scaffolds was significantly higher ($p < 0.001$) compared with cast films and coverslips. Furthermore, cell proliferation on the electrospun scaffolds was very fast, which might be a consequence of higher porosity and larger surface area to volume available for cell attachment. The groove on the surface of each fiber (shown in Fig. 4), appears to be a favorable parameter for cell attachment and proliferation.[22,23] Thus, this study demonstrated that surface topography affected cell attachment and proliferation.

Cell morphology and the interaction between cells and electrospun SF scaffolds were studied *in vitro* for 1 and 7 days. SEM micrographs are shown in Figure 10. After 1 day, PEICs had attached and spread on the surface of SF scaffolds, and after 7 days of culturing, the cells on the fibrous scaffolds almost completely occupied the entire surface and formed a typical confluent endothelial monolayer. Such ultrafine fibrous scaffolds may be advantageous for endothelial cells seeding or vascularization of scaffolds for tissue engineering. Wang et al.[24] have shown that the degradation rate and tissue ingrowth of SF scaffolds from all-aqueous solutions were faster than that from an organic solvent (HFIP). Electrospun SF scaffolds from aqueous solutions are appropriate for developing an endothelial cell layer and thus have potential application in vascular tissue engineering.

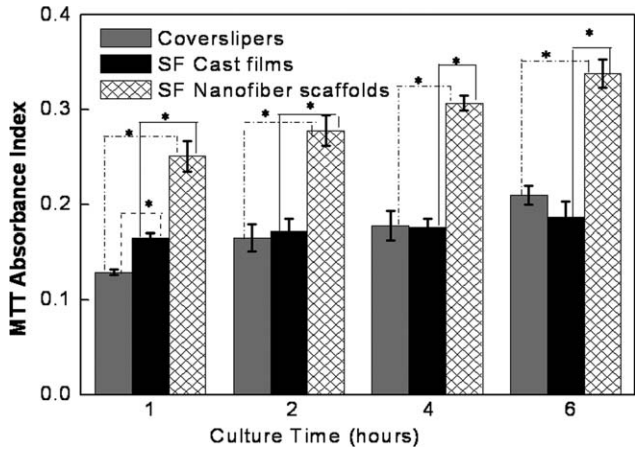


**Figure 8.** Attachment of PEICs cultured on SF fibrous scaffolds, SF cast films, and coverslips for 1, 2, 4, and 6 h. Data are expressed as mean ± SD ($n = 3$). Statistical difference between groups is indicated (*$p < 0.001$).

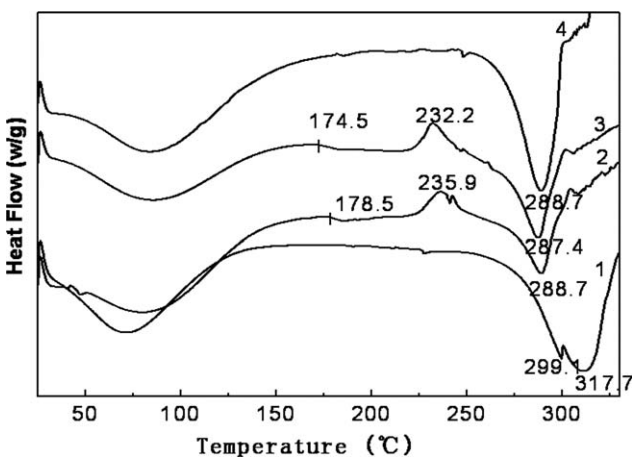


**Figure 7.** DSC thermographs of SF matrices. 1-degummed silk, 2-lyophilized sponge, 3-electrospun scaffolds, and 4-electrospun scaffolds treated with methanol.

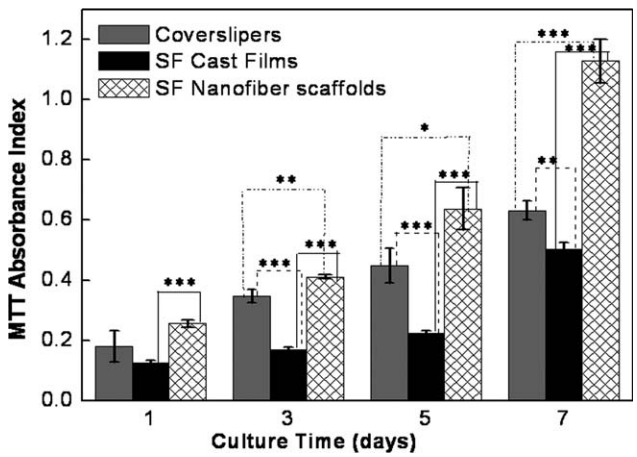


**Figure 9.** Proliferation of PEICs cultured on SF fibrous scaffolds, SF cast films, and coverslips for 1, 3, 5, and 7 days. Data are expressed as mean ± SD ($n = 3$). Statistical difference between groups is indicated (*$p < 0.05$; **$p < 0.01$; ***$p < 0.001$).

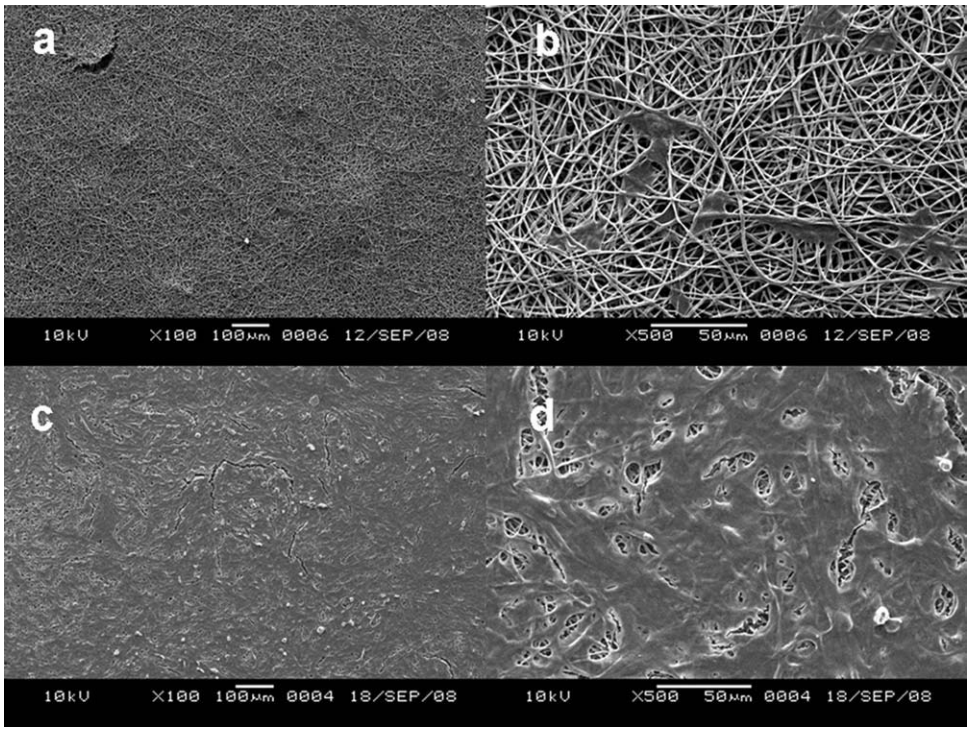


**Figure 10.** SEM micrographs of PEICs grown on the fibrous scaffolds. (a,b) 1 day and (c,d) 7 days.

## CONCLUSIONS

In this study, ultrafine SF fibers with average widths between 234 and 1016 nm were formed from SF aqueous solutions through electrospinning. Interestingly, there was a groove on the surface of fiber after treated with methanol, and such kind of surface topography was conducive to cell attachment and growth when compared with cast films and coverslips. Electrospun SF scaffolds have the potential of application for cardiovascular tissue engineering.

## References

1. Santin M, Motta A, Freddi G, Cannas M. In vitro evaluation of the inflammatory potential of the silk fibroin. J Biomed Mater Res 1999;46:382–389.
2. Horan RL, Antle K, Collette AL, Wang YZ, Huang J, Moreau JE, Volloch V, Kaplan DL, Altman GH. In vitro degradation of silk fibroin. Biomaterials 2005;26:3385–3393.
3. Zarkoob S, Eby RK, Reneker DH, Hudson SD, Ertley D, Adams WW. Structure and morphology of electrospun silk nanofibers. Polymer 2004;45:3973–3977.
4. Kawahara Y, Nakayama A, Matsumura N, Yoshioka T, Tsuji M. Structure for electro-spun silk fibroin nanofibers. J Appl Polym Sci 2008;107:3681–3684.
5. Ohgo K, Zhao CH, Kobayashi M, Asakura T. Preparation of non-woven nanofibers of *Bombyx mori* silk. Samia cynthia ricini silk and recombinant hybrid silk with electrospinning method. Polymer 2003;44:841–846.
6. Sukigara S, Gandhi M, Ayutsede J, Micklus M, Ko F. Regeneration of *Bombyx mori* silk by electrospinning. I. Processing parameters and geometric properties. Polymer 2003;44:5721–5727.
7. Kim KH, Jeong L, Park HN, Shin SY, Park WH, Lee SC, Kim TI, Park YJ, Seol YJ, Lee YM, Ku Y, Rhyu IC, Han SB, Chung CP. Biological efficacy of silk fibroin nanofiber membranes for guided bone regeneration. J Biotechnol 2005;120:327–339.
8. Jin HJ, Fridrikh SV, Rutledge GC, Kaplan DL. Electrospinning *B. mori* silk with poly(ethylene oxide). Biomacromolecules 2002;3:1233–1239.
9. Zhang XH, Baughman CB, Kaplan DL. In vitro evaluation of electrospun silk fibroin scaffolds for vascular cell growth. Biomaterials 2008;29:2217–2227.
10. Chen C, Cao CB, Ma XL, Tang Y, Zhu HS. Preparation of non-woven scaffolds from all-aqueous silk fibroin solution with electrospinning method. Polymer 2006;47:6322–6327.
11. Zhu JX, Shao HL, Hu XC. Morphology and structure of electrospun scaffolds from regenerated silk fibroin aqueous solutions with adjusting pH. Int J Biol Macromol 2007;41: 469–474.
12. Wang H, Zhang YP, Shao HL, Hu XC. A study on the flow stability of regenerated silk fibroin aqueous solution. Int J Biol Macromol 2005;36:66–70.
13. Koombhongse S, Liu WX, Reneker DH. Flat polymer ribbons and other shapes by electrospinning. J Polym Sci Part B: Polym Phys 2001;39:2598–2606.
14. Deitzel JM, Kleinmeyer J, Harris D, Tan NCB. The effect of processing variables on the morphology of electrospun nanofibers and textiles. Polymer 2001;42:261–272.
15. Rahul S, Stephanopoulos G, Wang DIC. Review: Effects of substratum morphology on cell physiology. Biotechnol Bioeng 1994;43:764–771.
16. Chen X, Shao ZZ, Marinkovic NS, Miller LM, Zhou P, Chance MR. Conformation transition kinetics of regenerated

*Bombyx mori* silk fibroin membrane monitored by time-resolved FTIR spectroscopy. Biophys Chem 2001;89:25–34.
17. Zhou P, Li GY, Shao ZZ, Pan XY, Yu TY. Structure of *Bombyx mori* silk fibroin based on the DFT chemical shift calculation. J Phys Chem B 2001;105:12469–12476.
18. Ruan QX, Zhou P. Sodium ion effect on silk fibroin conformation characterized by solid-state NMR and generalized 2D NMR-NMR correlation. J Mol Struct 2008;883:85–90.
19. Asakura T, Kuzuhara A, Tabeta R, Saito H. Conformation characterization of *Bombyx mori* silk fibroin in the solid state by high-frequency $^{13}C$ cross polarization-magic angle spinning NMR. X-ray diffraction, and infrared spectroscopy. Macromolecules 1985;18:1841–1845.
20. Magoshi J, Magoshi Y, Nakamura S, Kasai N, Kakudo M. Physical properties and structure of silk. V. Thermal behavior of silk fibroin in the random-coil conformation. J Polym Sci Polym Phys Ed 1977;15:1675–1683.
21. Lutolf MP, Hubbell JA. Synthetic biomaterials as instructive extracellular microenvironments for morphogenesis in tissue engineering. Nat Biotechnol 2005;23:47–55.
22. Teixeira AI, Nealey PF, Murphy CJ. Responses of human keratocytes to micro- and nano structured substrates. J Biomed Mater Res 2004;71A:369–376.
23. Curtis A, Wilkinson C. New depths in cell behaviour: Reactions of cells to nanotopography. Biochem Soc Symp 1999;65:15–26.
24. Wang YZ, Rudym DD, Walsh A, Abrahamsen L, Kim HJ, Kim HS, Kirker-Head C, Kaplan DL. In vivo degradation of three-dimensional silk fibroin scaffolds. Biomaterials 2008;29:3415–3428.